2023 45th Annual International Conference of the IEEE Engineering in Medicine & Biology Society (EMBC) | 979-8-3503-2447-1/23/$31.00 ©2023 IEEE | DOI: 10.1109/EMBC40787.2023.10340337

Reactive-Accelerated-Aging Testing of Thinned Tissue-Engineered Electronic Nerve Interfaces

Ladan Jiracek-Sapieha[1,2], *Member, IEEE*, Kenneth Fluker, Jr[1,2]., and Jack Judy[1,2,3,4], Senior *Member, IEEE*
[1]*Nanoscience Institute for Medical and Engineering Technology (NIMET),*
[2]*Department of Electrical and Computer Engineering,* [3]*Department of Biomedical Engineering,*
[4]*Department of Neurology University of Florida*

***Abstract*— Tissue responses can cause a significant reduction in the performance of microelectrode-based devices implanted into neural tissue. Since the reduction of the thickness of implants has been shown to reduce tissue response, in this work we report on our effects to reduce the thickness of our tissue-engineered-electronic-nerve-interface (TEENI) devices and characterize their long-term reliability in a harsh environment. We were able to reduce the thickness of the TEENI threads that are to be located in nerve tissue from ∼10 μm to ∼2.5 μm in total thickness. To maintain the handleability needed during the assembly of the TEENI device into the hydrogel-based scaffold, we maintained full thickness elsewhere in the TEENI device and added support rails. During longitudinal reactive-accelerated-aging (RAA) experiments performed over 6 days and at 67°C, which corresponds to ∼48 days in tissue, we observed that some channels maintain a stable impedance and others do not. Although analyses performed using a scanning electron microscope could clearly reveal delamination in some channels that exhibited large changes in impedance, it did not always correlate. Some channels with significant changes in impedance did not exhibit any observable delamination. Additional work is needed to study the relationship between changes in impedance and structural changes in the device, with the goal of improving device design to achieve longer-lasting devices.**

I. Introduction

The combined prevalence of traumatic unilateral and bilateral upper-limb amputation in the United States and across the globe are estimated to be ∼2 M and 22.3 M respectively [5]. Such limb amputation is a major life event that negatively impacts quality of life for many years after the operation. Although prosthetic limbs can be used to restore some lost function, the amount of function restored is related to the prosthetic limb technology, the control interface, and patient acceptance. Advanced upper prosthetic limbs can have more than 20 degrees of mechanical freedom and some even include the delivery of sensory information directly to neural tissue as well [6]. Unfortunately, advances in neural interfaces to control the prostheses have not kept pace with limb-technology improvements. To control state-of-the-art prosthetic limbs with speed and precision and provided high-resolution sensory percepts, a new bidirectional nerve-interface that can reliably interface with many independent motor and sensory channels is needed. In prior work, we reported on the development of a new type of regenerative neural interface that integrates arrays of microfabricated electrodes into a tissue-engineered scaffold. When the tissue-engineered electronic nerve interface (TEENI) is sutured to a nerve stump, the residual nerve stump grows through the scaffold towards a tissue target (e.g., a nerve stump innervating muscle tissue or de-innervated muscle tissue) [7] [1]. Unlike most neural interfaces that provide a 1-D or 2-D arrangement of electrodes inside motor nerves, a novelty of the TEENI interface technology is the design flexibility and scalability to enable a 3-D arrangement of microelectrodes to engage with a 3-D distribution of nodes of Ranvier in the regenerated nerve. However, in prior work, we demonstrated that a tissue response forms around each thread that could reduce the signal-to-noise ratio when recording action potentials [2]. In the effort described here, we were inspired by pioneering research that used much thinner and narrow threads to cause much less tissue response and achieve higher SNR recordings of action potentials [3] [4]. In the next sections we describe our approach to make the TEENI threads much thinner and narrower. Although our ultimate goal for the smaller TEENI threads is to cause a reduced tissue response and achieve higher SNR, in this work we focused on the impact of thinning on the long-term reliability of the smaller TEENI threads as tested with reactive accelerated aging.

II. Design

In initial attempts, we explored making TEENI devices with thinner polyimide throughout the entire device. Although it was possible to fabricate such thin devices, we found handling such thin devices very difficult. Given the amount of handling required during the assembly of the TEENI devices into the tissue-engineered scaffolds [2], we decided that a different approach was required. Instead of thinning the entire TEENI device, we decided to only thin the portions that would be located inside the nerve. However, since this would not completely alleviate the handleability issue (i.e., the device would still be subject to stretching or tangling) we added support rails parallel to the threads. Figure 1 clearly shows the change from our original TEENI

This work was sponsored by the Defense Advanced Research Projects Agency (DARPA) Biological Technology Office (BTO) Electrical Prescriptions (ElectRx) program under the auspices of Dr. Eric Van Gieson through the DARPA contracts Management Office, Pacific Cooperative Agreement: No. HR0011-15-2-0030.

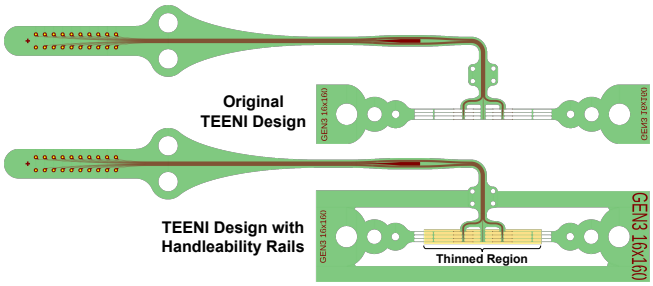

Fig. 1. Schematics diagrams of the design of the (top) original TEENI device and (bottom) new TEENI device. the new design includes a pair of wide support rails that were added to maintain the handleability the devices while the threads are thinned. The region of thinned threads is indicated by the yellow box.

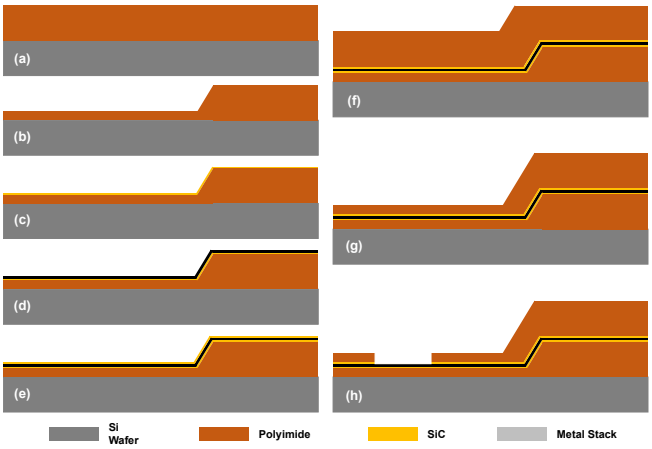

Fig. 2. Process flow for creating TEENI devices where only the threads are thinned.

design to that use in this work, where the selectively thinned region is indicated.

III. Fabrication

A. Device Fabrication

The multi-thickness TEENI devices were produced in a class 100-1000 cleanroom. The fabrication process begins with a blank 100-mm-diameter silicon (Si) wafer that is used as a carrier substrate. To prepare the substrate, organics and the native oxide layer are removed through soaks in piranha (i.e., sulfuric acid and hydrogen peroxide) and buffered oxide etch respectively. The native oxide layer is reapplied, and the wafer is coated with HMDS. A 5-μm-thick layer of polyimide (U-varnish S, UBE Ind.) is spun onto the wafer (Fig. 2a) and cured with maximum temperature of 450°C. After curing, a 11.4-μm-thick layer of positive photoresist (PR) (AZ 9260, MicroChemicals GmbH) is spun onto the wafer and patterned to define windows through which only the TEENI threads will be thinned. An oxygen-plasma based reactive-ion-etch (RIE) process is used to reduced the thickness of the first polyimide layer from 5 μm to 1.25 μm (Fig. 2b). Because the photoresist mask also etches during this process, the width of the openings through the PR mask will also increase. As a result, the sidewalls of the etched polyimide layer have a graduate slope that subsequent metal layers can cover while maintain electrical continuity. After the PR mask has been removed, the wafer is placed back into an RIE O_2 plasma for surface activation. Immediately after activation, a 250-nm-thick layer of silicon carbide (SiC) is deposited using PECVD (Unaxis 790, Plasma-Therm, LLC) at 300°C (Fig. 2c). Next, a 3-µm-thick layer of negative photoresist (nLOF 2035, MicroChemicals GmbH) is used as a lift-off mask, and a 400-nm-thick metal stack of Ti/Pt/Au/Pt/Ti (50 nm/100 nm/100 nm/100 nm/50 nm) is deposited by sputtering (CMS-18 multi-source, Kurt K. Lesker Company) (Fig. 2d). After metal deposition, the wafer is soaked in NMP at 70 °C and sonicated to lift off excess metal. Now that the metal layers have been defined, a second 250-nm-thick layer of SiC is deposited to encapsulate the metal features. A thin layer of positive photoresist (AZ1512, MicroChemicals GmbH) is deposited and then patterned to expose the SiC regions non on or immediately adjacent to the metal features (Fig. 2e). To etch through both SiC layers, an SF_6 RIE/ICP dry etch (Unaxis SLR, Plasma-Therm, LLC.) is used. After the PR mask is stripped, residual surface organics and fluorine are removed using an O_2 plasma etch. To promote adhesion, a thin layer of an aminopropyl triethoxysilane adhesion agent (VM-652, HD Microsystems) is deposited before a second 5-μm-thick layer of polyimide is spin-coated onto the wafer (Fig. 2f). As before, a 11.4-μm-thick layer of positive PR is spun onto the wafer and patterned to define a second set of tread-thinning regions and an O_2-plasma-based RIE is used to thin the second polyimide layer from 5 μm to 1.25 μm (Fig. 2g). After an 11.4-μm-thick positive PR is spun on and patterned to reveal the electrode sites and connector pads, an RIE dry etch with O_2 is used to etch through the polyimide, and an RIE/ICP SF_6 plasma is used to etch through the second SiC layer down to the metal stack (Fig. 2h). After a 150-nm-thick SiO_2 layer is deposited, a 1.5-µm-thick positive photoresist (AZ 9260, MicroChemicals GmbH) is patterned and the SiO_2 is etched using an SF_6 plasma. While using the patterned SiO_2 layer as a hard mask, an O_2 plasma etches through both polyimide layer to define the exterior geometry of the TEENI device. Lastly, the SiO_2 hard mask is removed from the devices using an SF_6 plasma and the TEENI devices are removed from the wafer using tweezers.

Cross section of thick to thin section shows metal continuity throughout the step meaning there were no shorts or opens within the electrical traces in this region.

B. Bonding and Packaging

To electrochemically characterize the TEENI devices and to perform longitudinal reactive accelerated aging, the TEENI device was attached to a long and narrow rigid printed-circuit board. To attach the TEENI device to the PCB, we used a wirebonder (K&S 4124 Ball Bonder) and 25 μm Au wire to form rivet-like ball bonds through each contact pad [9]. The other end of the circuit board is connected to a potentiostat through a multiplexer unit (MUX) that allowed the continuous measurement of all channels (4 devices).

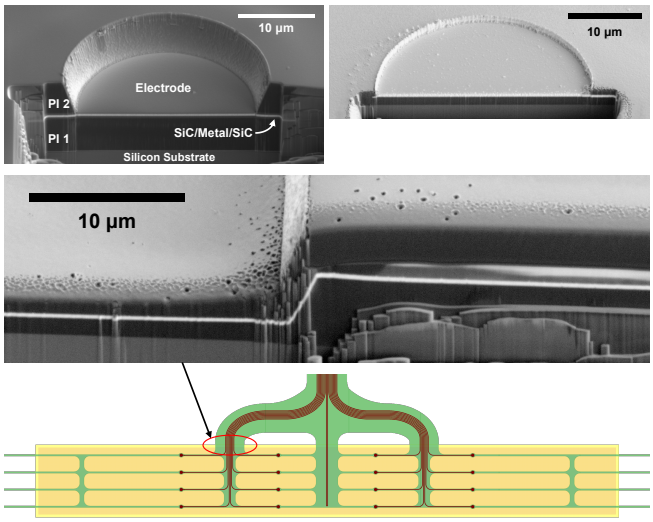

Fig. 3. SEM images of the cross sections of a (top left) full-thickness TEENI device and (top right) thinned TEENI device (2.5 μm total thickness). (middle) SEM image of the cross-section of a thinned TEENI device that illustrates the step in the polyimide layers and the metal covering it. (bottom) Illustration showing the location of the metal-step-coverage SEM.

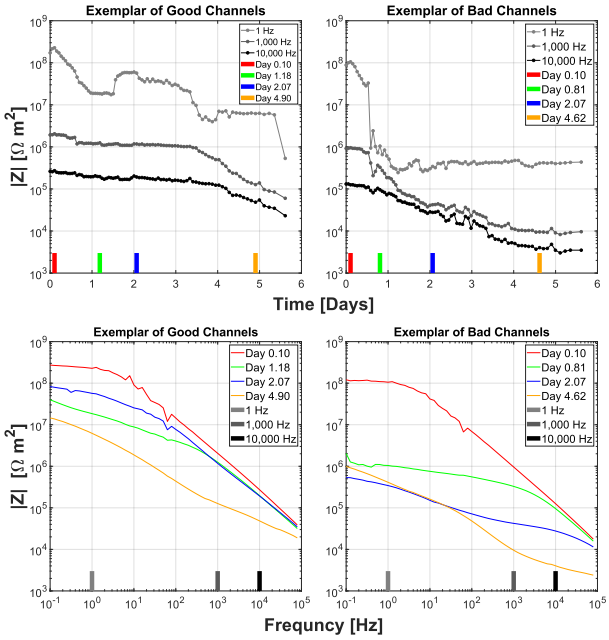

Fig. 4. (top) Plots of impedance measured longitudinally over 6 days for two different electrodes that act as exemplars of both good and bad channels. The plots only show the impedance measured at 1 Hz, 1 kHz, and 10 kHz. The vertical color bars indicate the time points at which full-bandwidth plots of impedance are provided in the next figure. (bottom) Plots of impedance measured at different time points for exemplars of both good and bad channels. The time point of each measurement is indicated by the color of the plot, which correspond to the vertical color based in the previous figure. The vertical grey bars indicate the frequencies show in the figure of the longitudinal impedance plots.

Finally, the connection between the TEENI device and the PCB as well as the rest of the PCB, except the contact pads used to connect to the MUX, are encapsulated in medical-grade silicone (Bluesil RTV 3040, Bluestar Silicone USA Corp.) using a 3-D printed mold.

IV. Characterization

To assess the long-term reliability of neural interfaces, accelerated soak testing is typically performed in heated saline solutions. However, the use of a reactive-accelerated-aging (RAA) soak test, which includes H_2O_2 to mimic reactive oxygen species, is argued to better match the environment that implanted devices experience [10], [11]. Our RAA experiments were performed using a potentiostat (PGSTAT302N, Metrohm Autolab) programmed to run electrical impedance spectroscopy (EIS) measurements. The EIS spectra were obtained using a 3-electrode setup, with the TEENI electrode acting as the working electrode ($n = 16$, per device), a Pt-wire counter as the electrode, and a 3 M KCl Ag/AgCl electrode as the reference electrode. The EIS experiments were performed with a 10 mV sinusoid, over a wide frequency range (0.1 Hz to 100 KHz), and with no dc offset with respect to the open circuit potential. The soak tests were performed in a 0.1 M concentration of phosphate-buffered saline (PBS) (P4417, Sigma Aldrich) that included 10 to 20 mM H_2O_2 at 67°C. Since the H_2O_2 degrades rapidly at 67°C, automated replenishment with concentrated H_2O_2 was used to maintain a constant concentration, which was verified using a titanium (IV) oxysulfate colorimetric assay. We used a 500 mL 5-neck round bottom flasks and a peristaltic pump to ensure a uniform H_2O_2 concentration and temperature. A heating mantle powered by a dc power supply (APS-3103, Aktakom) provided heat to the solution without introducing electrical noise.

We performed longitudinal EIS experiments for 6 days, which at 67°C correspond to approximately 48 days at body temperature. To observe possible changes in the electrochemical state of the devices tested over time, which could correspond to physical changes (e.g., delamination), we plotted the impedance measured at 1 Hz, 1 kHZ, and 10 kHz. Exemplars of good and bad channels are shown in Fig. 4. The exemplar of the good channels exhibits stable impedances over time. Although the impedances of even the higher-frequency measurements also dropped by the end of the experiment, this is consistent with our experience when using RAA to challenge the reliability of polyimide-based neural interfaces. The exemplar of the bad channels exhibits the stereotypically observed rapid and significant downward change in impedance, which are assumed to be associated with localized delamination. Measurements performed at lower frequencies are more sensitive to changes and other perturbations and in some cases may anticipate failures in the future that are observed at higher frequencies. Changes in the full spectrum of the impedance for the exemplar channels are shown in Fig. **??** for selected time points.

A. SEM Study

Since it can be very difficult to observe delamination using a simple optical microscope, a destructive SEM analysis was performed. Specifically, we interrogate the microstructure of each device tested at the end of each RAA study.

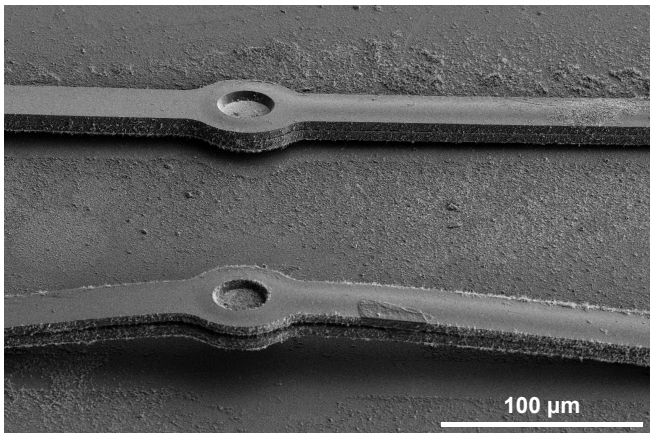

Fig. 5. SEM image of a pair of TEENI electrodes on adjacent threads that have been tested using RAA. The physical integrity of the upper thread is very good as it shows no delamination between the polyimide layers. The lower thread clearly illustrates delamination between the polyimide layers, which can be detected as changes in impedance.

The SEM image shown in Fig. 5 shows the observed difference between channels that experienced delamination and channels that did not. However, SEM analysis was not always definitive. In some cases, we did not observe any visual delamination present with channels that we did observe significant changes in the impedance using EIS. Additional experiments will be needed to further examine the relationship between changes in impedance with changes in the structure of the TEENI device.

V. Conclusions

To reduce the tissue response observed with TEENI devices, a reduction in the thickness of the TEENI threads is hypothesized to improve outcomes. To avoid extremely challenging handleability issues during assembly of the TEENI device, we only thinned the threads that will be located inside the nerve and added support rails. We have successfully developed a fabrication process that can produce TEENI devices with threads that are 4 times thinner than our original design (i.e., reduced from $\sim$10 μm to $\sim$2.5 μm in total thickness) and yet maintain full thickness throughout the rest of the TEENI device. When performing RAA experiments, we observed that some channels (i.e., electrodes) performed well (i.e., maintain a stable impedance) over time, whereas others demonstrated rapid and large reductions in impedance. Although an SEM analysis clearly showed that some electrodes experience significant delamination and others did not, the SEM analysis was not always correlated to the changes in impedance observed during EIS measurements. Future experiments performed with test structures specifically designed to examine the dependence between changes in impedance and polyimide delamination, could inform efforts to improve the reliability of polyimide-based devices when tested with RAA and thus long-term *in vivo* experiments.

Acknowledgment

The microfabrication reported here was enabled by the facilities and staff of the University of Florida Research Services Centers.

References

[1] P. P. Vu, A. K. Vaskov, Z. T. Irwin, P. T. Henning, D. R. Lueders, A. T. Laidlaw, A. J. Davis, C. S. Nu, D. H. Gates, R. Brent Gillespie, S. W. P. Kemp, T. A. Kung, C. A. Chestek, and P. S. Cederna, "A regenerative peripheral nerve interface allows real-time control of an artificial hand in upper limb amputees", Science Translational Medicine, vol. 12, no. 533, 2020.

[2] E. W. Atkinson, C. A. Kuliasha, M. Kasper, A. Furniturewalla, A. S. Lim, L. Jiracek-Sapieha, A. Brake, Anne Gormaley, V. Rivera-Llabres, I. Singh, B. Spearman, C. M. Rinaldi-Ramos, C. E. Schmidt, J. W. Judy, and K. J. Otto, "Examining the in vivo functionality of the magnetically aligned regenerative tissue-engineered electronic nerve interface (MARTEENI)", Journal of Neural Engineering, vol. 19, no. 5, 2022.

[3] P. R. Patel, H. Zhang, M. T. Robbins, J. B. Nofar, S. P. Marshall, M. J. Kobylarek, T. DY Kozai, N. A. Kotov, and C. A. Chestek, "Chronic in vivo stability assessment of carbon fiber microelectrode arrays", Journal of Neural Engineering, vol. 13, no. 6, 2016.

[4] Luan, Lan, Xiaoling Wei, Zhengtuo Zhao, Jennifer J. Siegel, Ojas Potnis, Catherine A. Tuppen, Shengqing Lin, S. Kazmi, R. A. Fowler, S. Holloway, A. K. Dunn, R. A. Chitwood, and C. Xie, "Ultraflexible nanoelectronic probes form reliable, glial scar–free neural integration", Science Advances, vol. 3, no. 2, 2017.

[5] C. L. McDonald, S. Westcott-McCoy, M. R. Weaver, J. Haagsma, and D. Kartin, "Global prevalence of traumatic non-fatal limb amputation", Prosthetics and Orthotics International, doi:10.1177/0309364620972258, 2020.

[6] J. A. George, D. T. Kluger, Tyler S. Davis, Suzanne M. Wendelken, E. V. Okorokova, Q. He, Christopher C. Duncan, D. T. Hutchinson, Z. C. Thumser, D. T. Beckler P. D. Marasco S. J. , and G. A. Clark, "Biomimetic sensory feedback through peripheral nerve stimulation improves dexterous use of a bionic hand", Science Robotics, vol. 4, no. 32, 2019.

[7] T. A. Kuiken, G. Li, B. A. Lock, R. D. Lipschutz, L. A. Miller, K. A. Stubblefield, and K. B. Englehart. "Targeted muscle reinnervation for real-time myoelectric control of multifunction artificial arms", JAMA, vol. 301, no. 6, pp. 619-628, 2009.

[8] C. A. Kuliasha and J. W. Judy, "The Materials Science Foundation supporting the microfabrication of reliable polyimide–metal neuroelectronic interfaces," Advanced Materials Technologies, vol. 6, no. 6, p. 2100149, 2021.

[9] T. Stieglitz,, H. Beutel, and J. Meyer. ""Microflex"—A new assembling technique for interconnects", Journal of Intelligent Material Systems and Structures, vol. 11, no. 6, pp. 417-425, 2000.

[10] P. Takmakov, K. Ruda, K. S. Phillips, I. S. Isayeva, V. Krauthamer, and C. G. Welle, "Rapid evaluation of the durability of cortical neural implants using accelerated aging with reactive oxygen species", J. Neural Eng., vol. 12, 2015.

[11] C. A. Kuliasha and J. W. Judy, "In Vitro Reactive-Accelerated-Aging (RAA) Assessment of Tissue-Engineered Electronic Nerve Interfaces (TEENI)", International Conference of the IEEE Engineering in Medicine and Biology Society (EMBC'18), pp. 1–4, 2018.